

$\text{CH}_3\text{C}_6\text{H}_4\text{NC})_3(\text{PPh}_3)_2\text{BPh}_4$ , 53111-61-8;  $[\text{FeCl}(4\text{-CH}_3\text{C}_6\text{H}_4\text{NC})_3(\text{PPh}_3)_2]\text{FeCl}_4$ , 53111-62-9;  $[\text{Fe}(\text{C}_6\text{H}_{11}\text{NC})_3(\text{PPh}(\text{OEt})_2)_3](\text{ClO}_4)_2$ , 53111-64-1;  $[\text{FeCl}(4\text{-CH}_3\text{C}_6\text{H}_4\text{NC})_5]\text{ClO}_4$ , 26201-85-4;  $[\text{FeCl}(\text{C}_6\text{H}_5\text{NC})_3]\text{ClO}_4$ , 53111-66-3;  $[\text{FeCl}_2(4\text{-CH}_3\text{-C}_6\text{H}_4\text{NC})_4]$ , 53111-67-4;  $\text{PPh}_3$ , 603-35-0.

### References and Notes

- (1) To whom correspondence should be addressed.
- (2) For a review see L. Malatesta and F. Bonatti, "Isocyanide Complexes of Metals," Wiley, New York, N. Y., 1969, pp 97-130.
- (3) L. Malatesta, *Gazz. Chim. Ital.*, **77**, 240 (1947).
- (4) C. Taylor and W. D. Horrocks, Jr., *Inorg. Chem.*, **3**, 584 (1964).
- (5) E. Bordignon, U. Croatto, U. Mazzi, and A. A. Orio, *Inorg. Chem.*, **13**, 935 (1974).
- (6) R. Rabinowitz and J. Pellon, *J. Org. Chem.*, **20**, 4623 (1961).
- (7) (a) I. Ugi, U. Fetzer, U. Eholzer, H. Knupfer, and K. Offerman, *Angew. Chem., Int. Ed. Engl.*, **4**, 672 (1965); (b) I. Ugi, and R. Meyer, *Org. Syn.*, **41**, 101 (1961).

- (8) (a) W. P. Weber and G. W. Gokel, *Tetrahedron Lett.*, **17**, 1637 (1972); (b) W. P. Weber, G. W. Gokel, and I. Ugi, *Angew. Chem., Int. Ed. Engl.*, **11**, 530 (1972).
- (9) (a) D. F. Evans, *J. Chem. Soc.*, 2003 (1959); (b) R. A. Bailey, *J. Chem. Educ.*, **49**, 297 (1972).
- (10) B. N. Figgis and J. Lewis, "Modern Coordination Chemistry," J. Lewis and R. G. Wilkins, Eds., Interscience, New York, N. Y., 1960, p 403.
- (11) G. Booth and J. Chatt, *J. Chem. Soc.*, 2099 (1962).
- (12) C. A. Tolman, *J. Amer. Chem. Soc.*, **92**, 2956 (1970).
- (13) C. A. Tolman, *J. Amer. Chem. Soc.*, **92**, 2953 (1970).
- (14) F. Bonatti and G. Minghetti, *J. Organometal. Chem.*, **22**, 195 (1970).
- (15) L. Malatesta, A. Sacco, and G. Padoa, *Ann. Chim. (Rome)*, **43**, 617 (1953).
- (16) W. D. Horrocks, Jr., and R. H. Mann, *Spectrochim. Acta*, **19**, 1375 (1963).

Contribution from the Department of Chemistry, Worcester Polytechnic Institute, Worcester, Massachusetts 01609

## $t_{2g}(\pi^*)$ Electron Distribution in Some Low-Spin Mixed-Ligand Complexes of Iron(III)

P. B. MERRITHEW,\* C.-C. LO, and A. J. MODESTINO

Received April 22, 1974

AIC40262O

The temperature dependence of the quadrupole splitting of  $[\text{Fe}(\text{bipy})_2(\text{CN})_2]\text{ClO}_4$ ,  $[\text{Fe}(\text{phen})_2(\text{CN})_2]\text{ClO}_4$ ,  $\text{H}[\text{Fe}(\text{bipy})(\text{CN})_4]\cdot 2\text{H}_2\text{O}$ , and  $\text{H}[\text{Fe}(\text{phen})(\text{CN})_4]\cdot 2\text{H}_2\text{O}$  was obtained in the range 80–300°. Electron paramagnetic resonance spectra were obtained at 77° on pure samples of these complexes. These data were interpreted to give the magnitude of the spin-orbit coupling constant and the splitting of the  $t_{2g}(\pi^*)$  orbitals. The results are found to be consistent with earlier studies of  $\text{K}_3\text{Fe}(\text{CN})_6$  and  $\text{Fe}(\text{bipy})_3(\text{ClO}_4)_3$ .

Numerous low-spin ( $S = 1/2$ ) iron(III) complexes of the form  $[\text{FeA}_6]^{1-3}$  and  $[\text{FeB}_3]^{3-9}$  where B is a bidentate ligand, have been studied by Mossbauer spectroscopy in an effort to characterize the cubic  $t_{2g}(\pi^*)$  (or  $t_{2g}(\pi)$ ) if the ligands are considered as back-bonding orbitals. The relative energies of the cubic  $t_{2g}(\pi^*)$  orbitals in high-spin ( $S = 2$ ) mixed-ligand complexes of iron(II) have also been extensively investigated by Mossbauer spectroscopy.<sup>10-12</sup> Until recently little attention had been paid to mixed-ligand complexes of iron(III). Reiff and DeSimone,<sup>13</sup> in an electron paramagnetic resonance (epr) and magnetically perturbed Mossbauer spectral study of  $[\text{Fe}(\text{bipy})_2(\text{CN})_2]^+$  (bipy = 2,2'-bipyridine) and  $[\text{Fe}(\text{phen})_2(\text{CN})_2]^+$  (phen = 1,10-phenanthroline), suggested that the complexes exhibit trigonal distortions. We have investigated the epr spectra, Mossbauer spectroscopy quadrupole splitting data, and magnetic susceptibilities of the compounds  $[\text{Fe}(\text{bipy})_2(\text{CN})_2]\text{ClO}_4$ ,  $[\text{Fe}(\text{phen})_2(\text{CN})_2]\text{ClO}_4$ ,  $\text{H}[\text{Fe}(\text{bipy})(\text{CN})_4]\cdot 2\text{H}_2\text{O}$ , and  $\text{H}[\text{Fe}(\text{phen})(\text{CN})_4]\cdot 2\text{H}_2\text{O}$  in an attempt to characterize the perturbation of the cubic  ${}^2T_{2g}$  ground term of these complexes.

### Experimental Section

**Preparation of Compounds.** The compounds  $[\text{Fe}(\text{bipy})_2(\text{CN})_2]\text{ClO}_4$ ,  $[\text{Fe}(\text{phen})_2(\text{CN})_2]\text{ClO}_4$ ,  $[\text{Fe}(\text{bipy})_2(\text{CN})_2]\text{NO}_3$ ,  $[\text{Fe}(\text{phen})_2(\text{CN})_2]\text{NO}_3\cdot 4\text{H}_2\text{O}$ ,  $\text{H}[\text{Fe}(\text{bipy})(\text{CN})_4]\cdot 2\text{H}_2\text{O}$ , and  $\text{H}[\text{Fe}(\text{phen})(\text{CN})_4]\cdot 2\text{H}_2\text{O}$  were prepared according to the methods of Schilt.<sup>14</sup>

**Physical Measurements.** The Mossbauer spectrometer and associated cryostat have been described previously.<sup>2</sup> The reproducibility of the spectrometer over the period of a typical sample run (24 hr) is better than 0.5%. The spectrometer was calibrated by employing  $\text{Na}_2[\text{Fe}(\text{CN})_5\text{NO}]\cdot 2\text{H}_2\text{O}$  as a standard with the quadrupole splitting taken as 1.726 mm/sec. The spectra were fitted with a least-squares program and the relative error was determined statistically.<sup>15</sup> It is this error which is given in Table I. The absolute error, due to inadequacies in the calibration procedure, is estimated to be less than 1%.

The epr spectra of  $[\text{Fe}(\text{bipy})_2(\text{CN})_2]\text{ClO}_4$  and  $\text{H}[\text{Fe}(\text{bipy})(\text{CN})_4]\cdot 2\text{H}_2\text{O}$  were obtained on instrumentation described previously.<sup>9</sup> A Varian E-9 spectrometer system at X-band frequency was employed

Table I. Quadrupole Splitting Data

Temp, °K	Quadrupole splitting, mm/sec	Temp, °K	Quadrupole splitting, mm/sec
$[\text{Fe}(\text{bipy})_2(\text{CN})_2]\text{ClO}_4$			
81 ± 2	1.72 ± 0.02	177	1.71 ± 0.01
96	1.73 ± 0.01	243	1.67 ± 0.02
105	1.73 ± 0.01	273	1.64 ± 0.01
119	1.73 ± 0.01	298	1.61 ± 0.01
145	1.72 ± 0.01		
$[\text{Fe}(\text{phen})_2(\text{CN})_2]\text{ClO}_4$			
81	1.55 ± 0.03	133	1.51 ± 0.02
83	1.55 ± 0.02	177	1.47 ± 0.03
96	1.55 ± 0.02	234	1.41 ± 0.03
101	1.54 ± 0.02	272	1.38 ± 0.03
116	1.53 ± 0.02	298	1.37 ± 0.01
$[\text{Fe}(\text{bipy})_2(\text{CN})_2]\text{NO}_3$			
81	1.75 ± 0.01	183	1.72 ± 0.02
118	1.74 ± 0.01	218	1.69 ± 0.01
123	1.74 ± 0.01	244	1.65 ± 0.02
157	1.74 ± 0.02	296	1.60 ± 0.02
$[\text{Fe}(\text{phen})_2(\text{CN})_2]\text{NO}_3\cdot 4\text{H}_2\text{O}$			
81	1.65 ± 0.02	192	1.58 ± 0.02
90	1.65 ± 0.01	240	1.55 ± 0.02
123	1.64 ± 0.01	271	1.51 ± 0.02
172	1.60 ± 0.02	295	1.49 ± 0.02
$\text{H}[\text{Fe}(\text{bipy})(\text{CN})_4]\cdot 2\text{H}_2\text{O}$			
81	1.63 ± 0.01	201	1.54 ± 0.01
95	1.63 ± 0.01	233	1.51 ± 0.01
103	1.62 ± 0.01	262	1.47 ± 0.01
124	1.60 ± 0.01	279	1.43 ± 0.01
144	1.59 ± 0.01	298	1.39 ± 0.01
173	1.56 ± 0.01		
$\text{H}[\text{Fe}(\text{phen})(\text{CN})_4]\cdot 2\text{H}_2\text{O}$			
93	1.45 ± 0.01	185	1.35 ± 0.01
103	1.44 ± 0.01	212	1.31 ± 0.01
113	1.43 ± 0.01	242	1.27 ± 0.02
160	1.39 ± 0.01	271	1.21 ± 0.02

to obtain spectra of  $[\text{Fe}(\text{phen})_2(\text{CN})_2]\text{ClO}_4$  and  $\text{H}[\text{Fe}(\text{phen})(\text{CN})_4]\cdot 2\text{H}_2\text{O}$ . All spectra were of pure powdered samples at 77°.

## Theory

**Quadrupole Splitting.** The quadrupole splitting,  $\Delta E$ , for  $^{57}\text{mFe}$  is

$$E = 1/2 e^2 q Q [1 + 1/3 \eta^2]^{1/2}$$

where  $Q$  is the quadrupole moment of the nucleus and  $q$  and  $\eta$  are functions of the components of the electric field gradient (EFG) tensor.<sup>16</sup> The quantities  $q$  and  $\eta q$  may be expressed<sup>11</sup>

$$q = q_d + q_i$$

$$\eta q = \eta_d q_d + \eta_i q_i$$

where the subscript d refers to temperature-dependent contributions and i to temperature-independent contributions. Asymmetries in the  $t_{2g}(\pi^*)$  (or  $t_{2g}(\pi)$  if the ligands are considered as back-bonding) electron distribution produce contributions to  $q_d$  and  $\eta_d$ . Charge asymmetries in the bonding orbitals give contributions to  $q_i$  and  $\eta_i$ .

The wave functions which describe the cubic  ${}^2T_{2g}$  term under simultaneous perturbation by spin-orbit coupling and a low-symmetry field may be obtained by solving a  $6 \times 6$  matrix similar to those which have been given before.<sup>1,3,17,18</sup> The distortion parameters are defined in the following manner. The axial splitting of the cubic  ${}^2T_{2g}$  term is  $\Delta$ . A positive  $\Delta$  indicates an orbitally nondegenerate ground term. (This convention is opposite to that employed by Reiff.<sup>13</sup> For a tetragonal distortion this would correspond to a  ${}^2B_{2g}$  ground term with the "hole" in an  $xy$  orbital.) The  ${}^2E_g$  term which arises from the axial splitting of the cubic  ${}^2T_{2g}$  term may be split by low-symmetry components. This splitting is  $\epsilon$ . The single electron spin-orbit coupling constant is  $\zeta$ .

The quantities  $q_d$  and  $\eta_d$  are calculated from the six wave functions by applying the usual methods.<sup>1,3,16</sup> As in previous treatments of low-spin ferric ions, the magnitude of  $2/7e^2Q(1-R)\langle r^{-3} \rangle$  was taken as 4.0 mm/sec.<sup>1,2,9</sup> In order to account for anisotropies in the radial parts of the  $t_{2g}(\pi^*)$  orbitals, the radial factor for the unique basis function was taken as  $\beta^2 \langle r^{-3} \rangle_0$  and that for the remaining functions as  $\alpha^2 \langle r^{-3} \rangle_0$ . (When the primary distortion is tetragonal, the unique orbital is  $xy$ ; when the primary distortion is trigonal, the unique orbital is  $z^2$ .) The magnitudes of  $\beta^2$  and  $\alpha^2$  reflect the reduction of the quantity  $2/7e^2Q(1-R)\langle r^{-3} \rangle_0$  from 4.0 mm/sec.

It is also possible to make some estimates of the sign and magnitude of the temperature-independent or "lattice" contributions to the EFG tensor. Since the asymmetry parameter,  $\eta$ , involves a ratio of the components of the EFG tensor,<sup>16</sup> the magnitude of  $\eta_i$  can be estimated from the symmetry of the molecule. Recognizing that the ligands will exhibit different  $\sigma$ -bonding strengths, 2,2'-bipyridine and  $\text{CN}^-$  are assigned different formal charges. The asymmetry parameter is then calculated by employing the usual formulas.<sup>19</sup> (It is probably reasonable to separate  $\sigma$ - from  $\pi$ -bonding effects here because the octahedral field splitting ( $>25,000 \text{ cm}^{-1}$ ) is much larger than the axial splitting of the ground term ( $<1200 \text{ cm}^{-1}$ ). The  $\pi$ -bonding effects need not be considered for this case since  $\pi$ -bonding affects the cubic  $t_{2g}(\pi)$  orbitals and therefore has an effect on only the temperature-dependent or "valence" contributions to the EFG tensor.) This simple point charge approach has been shown to be consistent with a more rigorous molecular orbital approach.<sup>20</sup> Employing similar logic several authors correctly predicted that the quadrupole splitting of the cis and trans isomers of some low-spin ( $S = 0$ ) ferrous complexes should show a -1:2 ratio.<sup>20-22</sup> If the relative  $\sigma$ -bonding strengths are known, then it is also possible to calculate the sign of  $q_i$ . A comparison of isomer shift data on a series of iron(II) low-spin compounds<sup>20</sup> suggests that cyanide is a stronger  $\sigma$  donor than 2,2'-bipyridine. Reiff and DeSimone,<sup>13</sup> employing the magnetic perturbation technique, determined

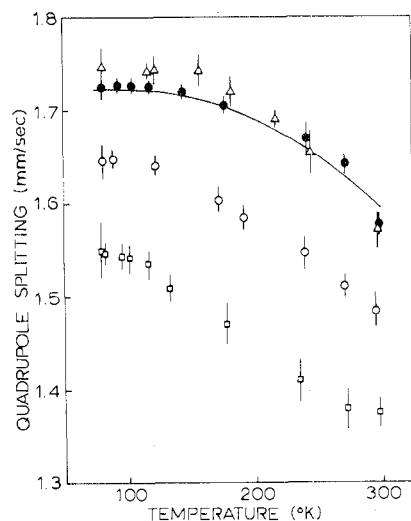


**Figure 1.** The temperature dependence of the quadrupole splitting: squares,  $[\text{Fe}(\text{phen})_2(\text{CN})_2]\text{ClO}_4$ ; circles,  $[\text{Fe}(\text{phen})_2(\text{CN})_2]\text{NO}_3 \cdot 4\text{H}_2\text{O}$ ; triangles,  $[\text{Fe}(\text{bipy})_2(\text{CN})_2]\text{NO}_3$ ; solid circles,  $[\text{Fe}(\text{bipy})_2(\text{CN})_2]\text{ClO}_4$ . The solid line gives a fitting with  $\zeta = 150 \text{ cm}^{-1}$ ,  $\Delta = 1000 \text{ cm}^{-1}$ ,  $\epsilon = 800 \text{ cm}^{-1}$ ,  $\beta^2 = 0.44$ , and  $1/2 e^2 Q \eta_i q_i = -0.40 \text{ mm/sec}$ .

that the low-spin iron(II) compound  $\text{Fe}(\text{bipy})_2(\text{CN})_2$  gives  $q$  as positive. This result is consistent with  $\text{CN}^-$  as a stronger  $\sigma$  donor than 2,2'-bipyridine. (If  $\pi$ -back-bonding effects predominated, a negative  $q$  would be expected.) The results of magnetic perturbation experiments on other mixed-ligand complexes are also consistent with  $\text{CN}^-$  as a relatively strong  $\sigma$  donor.<sup>21</sup>

**Epr.** The  $g$  values, in first order, may be calculated from the six wave functions which describe the  ${}^2T_{2g}$  term by following the procedure outlined by Griffith.<sup>18</sup> The  $g$  values, in first order, are a function of  $\Delta$ ,  $\epsilon$ ,  $\zeta$ , and a covalency parameter  $k$ .<sup>23</sup> Calculation of the  $g$  values to second-order requires a more complex calculation which has been described by Hill.<sup>24</sup> For the case of a tetragonal distortion from octahedral symmetry the formulas of Hill<sup>24</sup> are employed; for the trigonal case the formulas of Merrithew, Lo, and Modestino<sup>9</sup> are employed. Calculation of the  $g$  values to second order requires the Racah parameter,  $B$ , and an excitation energy,  $E$ .<sup>24</sup>

**Magnetic Susceptibility.** The temperature dependence of the average magnetic susceptibility can be calculated from the wave functions of the cubic  ${}^2T_{2g}$  ground term by employing the formula given by Van Vleck.<sup>25</sup> The temperature dependence of the average magnetic moment is in agreement with the results of Figgis.<sup>26</sup>

## Results and Discussion

The quadrupole splitting data are given in Table I and plotted in Figures 1 and 2. The room-temperature results are in reasonable agreement with those presented previously.<sup>13,27</sup> The bipyridine and phenanthroline compounds show a small difference in the magnitude of the quadrupole splitting but no significant difference in the temperature dependence. Examination of the data on the  $\text{Fe}(\text{phen})_2(\text{CN})_2^{2+}$  and  $\text{Fe}(\text{bipy})_2(\text{CN})_2^{2+}$  complexes suggests the magnitude of the quadrupole splitting is sensitive to the number of adducted water molecules.

The  $g$  values obtained from the epr spectra of pure powdered samples at 77° are shown in Table II. The large uncertainty in the  $g$  values is a result of the broad nature of the spectra. The epr spectra also show only a small difference between the bipyridine and phenanthroline complexes.

The compounds  $[\text{Fe}(\text{bipy})_2(\text{CN})_2]\text{ClO}_4$  and  $\text{H}[\text{Fe}(\text{bipy})(\text{CN})_4]$  have been chosen for theoretical analysis since both the epr and Mossbauer data of these compounds are of

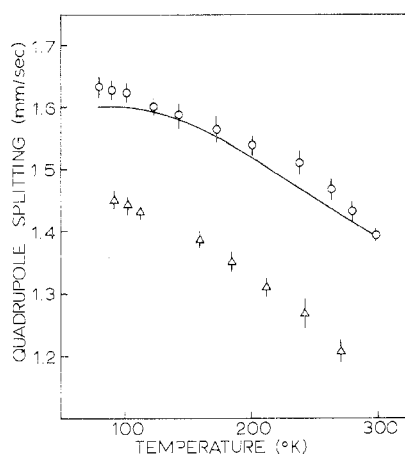


**Figure 2.** The temperature dependence of the quadrupole splitting: triangles,  $\text{H}[\text{Fe}(\text{phen})(\text{CN})_4] \cdot 2\text{H}_2\text{O}$ ; circles,  $\text{H}[\text{Fe}(\text{bipy})(\text{CN})_4] \cdot 2\text{H}_2\text{O}$ . The solid line gives a fitting with  $\zeta = 150 \text{ cm}^{-1}$ ,  $\Delta = -400 \text{ cm}^{-1}$ ,  $\epsilon = 400 \text{ cm}^{-1}$ ,  $\beta^2 = 0.28$ ,  $1/2e^2Qq_1 = 0.29 \text{ mm/sec}$ , and  $\eta_1 = -3$ .

**Table II**

Sample	$g_1, g_2$	$g_3$	Half-width, $g_1, \text{G}$
$[\text{Fe}(\text{bipy})_2(\text{CN})_2]\text{ClO}_4$	$2.50 \pm 0.05$ $2.30 \pm 0.05$	$2.00 \pm 0.05$	120
$[\text{Fe}(\text{phen})_2(\text{CN})_2]\text{ClO}_4$	$2.70 \pm 0.07$	$1.86 \pm 0.07$	150
$\text{H}[\text{Fe}(\text{bipy})(\text{CN})_4] \cdot 2\text{H}_2\text{O}$	$2.50 \pm 0.07$ $2.30 \pm 0.07$	$1.65 \pm 0.07$	130
$\text{H}[\text{Fe}(\text{phen})(\text{CN})_4] \cdot 2\text{H}_2\text{O}$	$2.7 \pm 0.2$	$1.6 \pm 0.1$	300

better quality. The results of this analysis should apply reasonably well to the phenanthroline compounds because of the similarity of the data.

**$[\text{Fe}(\text{bipy})_2(\text{CN})_2]\text{ClO}_4$ .** On the basis of epr, nmr, and magnetically perturbed Mossbauer spectral data Reiff and DeSimone<sup>13</sup> have suggested that the complexes  $[\text{Fe}(\text{bipy})_2(\text{CN})_2]^+$  and  $[\text{Fe}(\text{phen})_2(\text{CN})_2]^+$  exhibit trigonal distortions similar to those observed for the corresponding tris(diimine) systems. In trigonal quantization, the  $t_{2g}$  orbitals expressed in real form are  $|z^2\rangle$ ,  $(2/3)^{1/2}|x^2 - y^2\rangle - (1/3)^{1/2}|xz\rangle$  and  $(2/3)^{1/2}|xy\rangle + (1/3)^{1/2}|yz\rangle$ . Reiff and DeSimone have shown that the ground term is  $^2A$ , corresponding to a "hole" in the  $z^2$  orbital.

The temperature-independent or "lattice" contributions are treated in the manner described in the preceding section. Taking the principal  $z$  axis along the threefold axis of the octahedron, it is found that  $q_i \approx 0$  and the product  $\eta_i q_i$  is relatively large and negative. This conclusion, which appears inconsistent with the manner in which  $q$  and  $\eta$  are defined,<sup>19</sup> results from the fact that the major "lattice" contribution to the EFG tensor lies along a different axis from that of the major "valence" contribution.

The quadrupole splitting can be fitted in terms of only two of the six parameters:  $\zeta$ ,  $\Delta$ ,  $\epsilon$ ,  $\alpha^2$ ,  $\beta^2$ , and  $\eta_i q_i$ . A least-squares fitting program was employed to obtain the best fitting in terms of  $\beta^2$  and  $\eta_i q_i$  for various values of  $\zeta$  and  $\epsilon$  and positive values of  $\Delta$ . Initially it was assumed that  $\beta^2/\alpha^2 = 1.0$ . Those solutions which are in reasonable agreement (those for which the reduced  $\chi^2$  value  $\chi_r < 3$ ) with the quadrupole splitting are shown in Table III. The  $\beta^2$  value for all of these solutions is the same, with a magnitude of 0.39–0.45 with  $1/2e^2Q\eta_i q_i = -0.10$  to  $-1.40 \text{ mm/sec}$ . The solutions give  $q$  as positive and the asymmetry parameter,  $\eta$ , is 0.1–0.9. When the absolute magnitude of  $1/2e^2Q\eta_i q_i$  is relatively small ( $< 0.6$ ), the asymmetry parameter is small ( $< 0.3$ ) as expected on the basis of the results of Reiff and DeSimone.<sup>13</sup>

The expected  $g$  values for each of the Mossbauer spectroscopy solutions are shown in Table III. Results are shown

**Table III.** Sets of Parameters Which Give Reasonable Fittings to the Quadrupole Splitting Data of  $[\text{Fe}(\text{bipy})_2(\text{CN})_2]\text{ClO}_4$  and the Predicted  $g$  Values for These Solutions<sup>a</sup>

$\zeta$ , $\text{cm}^{-1}$	$\Delta$ , $\text{cm}^{-1}$	$\epsilon$ , $\text{cm}^{-1}$	$g_1$	$g_2$	$g_3$		
100	800	100	2.32 (2.18)	2.27 (2.16)	1.94 (1.95)		
		200	2.34 (2.20)	2.25 (2.14)	1.94 (1.95)		
		400	2.40 (2.24)	2.22 (2.12)	1.93 (1.94)		
		600	2.34 (2.20)	2.16 (2.09)	1.95 (1.96)		
		800	2.40 (2.24)	2.14 (2.07)	1.95 (1.95)		
		1000	2.34 (2.20)	2.11 (2.06)	1.96 (1.97)		
	1200	1000	2.40 (2.24)	2.10 (2.05)	1.95 (1.96)		
		1200	2.34 (2.20)	2.10 (2.06)	1.96 (1.97)		
		150	800	200	2.52 (2.30)	2.38 (2.21)	1.86 (1.88)
		400		2.61 (2.35)	2.33 (2.17)	1.85 (1.87)	
		700		2.56 (2.33)	2.23 (2.11)	1.89 (1.90)	
		1000	800	800	2.61 (2.36)	2.21 (2.10)	1.88 (1.89)
1000	2.52 (2.31)			2.25 (2.13)	1.89 (1.91)		
1200	2.61 (2.36)			2.15 (2.06)	1.89 (1.91)		
1200	800		200	2.68 (2.33)	2.50 (2.26)	1.75 (1.79)	
	400		2.79 (2.46)	2.49 (2.26)	1.73 (1.77)		
	800		2.95 (2.56)	2.20 (2.56)	1.73 (1.76)		
1200	1000	1000	2.69 (2.41)	2.22 (2.06)	1.84 (1.86)		
		1200	2.80 (2.48)	2.18 (2.06)	1.81 (1.84)		
		1400	2.74 (2.44)	2.14 (2.05)	1.85 (1.87)		
	1700	1500	2.87 (2.51)	2.10 (2.01)	1.81 (1.83)		

<sup>a</sup> The  $g$  values are calculated with  $B = 570 \text{ cm}^{-1}$ ,  $E = 25,000 \text{ cm}^{-1}$ , and  $\zeta_{\sigma\pi} = 160 \text{ cm}^{-1}$ . The two sets of  $g$  values are for  $k = 1.0$  and  $k = 0.6$  (in parentheses).

for both  $k = 0.6$  and  $k = 1.0$ . The Racah parameter,  $B$ , the excitation energy,  $E$ , and the spin-orbit coupling constant,  $\zeta_{\sigma\pi}$ , are taken as  $570 \text{ cm}^{-1}$ ,  $25,000 \text{ cm}^{-1}$ , and  $160 \text{ cm}^{-1}$ , respectively, the weighted averages of the values observed for  $\text{Fe}(\text{CN})_6^{3-}$ ,<sup>2,28</sup> and  $\text{Fe}(\text{bipy})_3^{3+}$ .<sup>29,30</sup> These values are somewhat arbitrary. In particular the value for  $\zeta_{\sigma\pi}$  may be considerably larger than  $160 \text{ cm}^{-1}$  since  $\langle r^{-3} \rangle_{e_g}$  may be larger than  $\langle r^{-3} \rangle_{t_{2g}}$ . ( $\zeta$  is proportional to  $\langle r^{-3} \rangle$ .)<sup>30</sup> Fortunately, the  $g$  values are not very sensitive to the magnitude of these quantities. The variation of the  $g$  values with  $k$ , as shown in Table III, represent reasonably well the variation that may be achieved by alteration of the parameters  $B$ ,  $E$ , and  $\zeta_{\sigma\pi}$ .

Examination of Table III reveals that reasonable agreement between the epr and quadrupole splitting results is obtained with  $\zeta \approx 150 \text{ cm}^{-1}$ , the ratio  $\Delta/\zeta \approx 7$ , and  $\epsilon$  somewhat smaller than  $\Delta$ . The agreement between the experimental and calculated  $g$  values is not entirely satisfactory. This lack of exact agreement does not result from any constraint imposed by the Mossbauer spectroscopy results. With  $k < 1.0$  no set of parameters can be found which exactly fit the epr data. The lack of perfect agreement may be a result of the inadequacies in the theoretical treatment.

The quadrupole splitting was also fitted with  $\beta^2/\alpha^2 \neq 1.0$ . This anisotropy does not significantly change the range of  $\zeta$ ,  $\Delta$ , and  $\epsilon$  which give reasonable fittings, but it does have a significant effect on the magnitude of  $\beta^2$ . With  $\beta^2/\alpha^2 = 1.15$ ,  $\beta^2 \approx 0.55$ , and with  $\beta^2/\alpha^2 = 0.85$ ,  $\beta^2 \approx 0.35$ . The data were also fitted allowing for a nonzero "lattice" contribution to the  $z$  component of the EFG tensor. The results obtained are similar to those observed when  $\beta^2/\alpha^2 \neq 1.0$ .

The results of this analysis appear to be in reasonable agreement with the previous treatments of  $\text{Fe}(\text{CN})_6^{3-}$  and  $\text{Fe}(\text{bipy})_3^{3+}$ . For  $\text{K}_3\text{Fe}(\text{CN})_6$  it was found that  $\zeta \approx 85 \text{ cm}^{-1}$  and  $\beta^2 \approx 0.15$ .<sup>2</sup> The corresponding values for  $\text{Fe}(\text{bipy})_3^{3+}$  are  $\zeta \approx 200 \text{ cm}^{-1}$  and  $\beta^2 \approx 0.50$ .<sup>9</sup> The results for  $[\text{Fe}(\text{bipy})_2(\text{CN})_2]\text{ClO}_4$ ,  $\zeta \approx 150 \text{ cm}^{-1}$  and  $\beta^2 \approx 0.40$  are close to a weighted average of the values observed for  $\text{Fe}(\text{CN})_6^{3-}$  and  $\text{Fe}(\text{bipy})_3^{3+}$ . The relatively small perturbation observed here probably accounts for the sensitivity of the quadrupole splitting and epr results to intermolecular effects. (The epr results of Reiff and DeSimone<sup>13</sup> obtained in frozen solution are different from those of the pure material.)

The temperature dependence of the average magnetic

Table IV. Sets of Parameters Which Give Reasonable Fittings to the Quadrupole Splitting Data of  $\text{H}[\text{Fe}(\text{bipy})(\text{CN})_4]$  and the Predicted  $g$  Values for These Solutions<sup>a</sup>

$\zeta, \text{cm}^{-1}$	$\Delta, \text{cm}^{-1}$	$\epsilon, \text{cm}^{-1}$	$\beta^2$	$1/2 e^2 Qq_1, \text{mm/sec}$	$g_1$	$g_2$	$g_3$	
100	-200	400	0.27	0.31	$g_1 \cong g_2$			
		600	0.31	0.20				
	-300	300	0.18	0.48	2.80 (2.45)	2.48 (2.24)	1.68 (1.74)	
		400	0.22	0.39	2.60 (2.35)	2.47 (2.47)	1.78 (1.82)	
		500	0.29	0.25	2.49 (2.28)	2.44 (2.25)	1.84 (1.87)	
	-400	300	0.20	0.44	2.80 (2.47)	2.38 (2.18)	1.72 (1.77)	
		400	0.25	0.32	2.62 (2.36)	2.38 (2.20)	1.80 (1.84)	
		500	0.33	0.16	2.50 (2.29)	2.37 (2.20)	1.85 (1.88)	
	-500	300	0.22	0.41	2.81 (2.47)	2.31 (2.14)	1.75 (1.79)	
		500	0.37	0.08	2.50 (2.29)	2.32 (2.17)	1.87 (1.89)	
	-600	300	0.23	0.38	2.81 (2.48)	2.26 (2.11)	1.77 (1.81)	
		500	0.41	0.01	2.50 (2.29)	2.27 (2.15)	1.88 (1.90)	
	400	400	0.48	0.38	2.62 (2.37)	2.27 (2.14)	1.84 (1.87)	
		600	-100	0.47	0.61			
	800	-300	0.43	0.80				
		-500	0.47	0.37	$g_3 > 1.85$			
		-700	0.42	0.01				
	150	-200	400	0.32	0.26	2.81 (2.42)	2.81 (2.42)	1.45 (1.54)
			600	0.36	0.14	2.71 (2.40)	2.57 (2.30)	1.69 (1.74)
		-400	300	0.24	0.40	3.11 (2.63)	2.49 (2.20)	1.43 (1.52)
400			0.28	0.29	2.88 (2.49)	2.53 (2.26)	1.61 (1.67)	
500			0.37	0.11	2.72 (2.40)	2.52 (2.27)	1.71 (1.75)	
-600		300	0.27	0.33	3.14 (2.66)	2.32 (2.09)	1.53 (1.60)	
		400	0.33	0.19	2.90 (2.52)	2.37 (2.16)	1.68 (1.73)	
-1000		400	0.38	0.10	2.90 (2.53)	2.21 (2.07)	1.74 (1.78)	
		-400	0.50	0.65	2.85 (2.47)	2.64 (2.32)	1.54 (1.62)	
-300		-500	0.49	0.60	2.70 (2.39)	2.62 (2.33)	1.66 (1.72)	
		-400	0.50	0.54	2.88 (2.49)	2.53 (2.26)	1.61 (1.67)	
-400		-500	0.49	0.43	2.72 (2.40)	2.52 (2.27)	1.71 (1.76)	
		-600	0.49	0.31	2.89 (2.52)	2.37 (2.17)	1.67 (1.73)	
700		600	0.48	0.28	2.90 (2.53)	2.28 (2.11)	1.72 (1.76)	
800		800	0.47	0.20	2.91 (2.53)	2.21 (2.07)	1.74 (1.78)	
500		-100	0.47	0.76	2.78 (2.43)	2.61 (2.31)	1.63 (1.69)	
		-200	0.45	0.83	2.88 (2.49)	2.53 (2.26)	1.61 (1.67)	
600		-100	0.49	0.57	2.65 (2.38)	2.54 (2.29)	1.73 (1.78)	
		-300	0.48	0.69	2.80 (2.46)	2.43 (2.21)	1.71 (1.76)	
800		-600	0.48	0.68	2.74 (2.43)	2.28 (2.13)	1.80 (1.83)	
	-800	0.42	0.89	2.91 (2.54)	2.21 (2.07)	1.78 (1.78)		
200	1000	-1000	0.47	0.26	$g_3 > 1.80$			
	-200	-100	0.91	0.50				
		-400	-100	0.79	0.22	$g_3 < 1.45$		
	-400	-400	0.54	0.48				
		-400	0.51	0.25	3.12 (2.64)	2.44 (2.16)	1.46 (1.54)	
	-800	-400	0.47	0.07	3.14 (2.66)	2.32 (2.09)	1.53 (1.60)	
	-200	400	0.31	0.32	$g_1 = g_2$			
		100	0.47	0.35	$g_3 < 1.45$			
	-400	400	0.35	0.21				
		-600	300	0.34	0.25	3.37 (2.79)	2.34 (2.05)	1.24 (1.35)
	-600	400	0.40	0.10	3.12 (2.64)	2.44 (2.16)	1.46 (1.55)	
		300	0.37	0.19	3.41 (2.83)	2.12 (1.92)	1.39 (1.47)	
	500	-100	0.52	0.73	2.95 (2.51)	2.74 (2.36)	1.37 (1.47)	
		-200	0.50	0.81	3.08 (2.59)	2.63 (2.27)	1.34 (1.45)	
	600	-100	0.52	0.48	2.83 (2.45)	2.67 (2.34)	1.55 (1.62)	
		-200	0.51	0.67	2.91 (2.51)	2.59 (2.29)	1.53 (1.61)	
	-400	-400	0.48	0.88	3.12 (2.64)	2.44 (2.17)	1.46 (1.55)	
		-600	0.51	0.42	2.95 (2.55)	2.34 (2.14)	1.66 (1.71)	
	800	-900	0.44	0.93	3.27 (2.75)	2.16 (1.98)	1.52 (1.56)	
		-1000	0.50	0.61	2.96 (2.56)	2.22 (2.07)	1.71 (1.76)	
1000	-1200	0.45	0.88	3.15 (2.68)	2.12 (1.98)	1.63 (1.68)		

<sup>a</sup> The  $g$  values are calculated with  $B = 650 \text{ cm}^{-1}$ ,  $E = 30,000 \text{ cm}^{-1}$ , and  $\zeta_{\text{O}^-} = 120 \text{ cm}^{-1}$ . The two sets of  $g$  values are for  $k = 1.0$  and  $k = 0.6$  (in parentheses).

susceptibility, derived in a manner similar to that of Figgis,<sup>26</sup> has been calculated for several of the solutions which are consistent with the epr and quadrupole splitting data. The predicted magnetic moments were then compared with the experimental results obtained from the literature.<sup>31</sup> The agreement is poor. Figure 3 compares some of the calculated susceptibilities with the experimental data. The poor agreement may be the result of an inadequate theoretical analysis. Gerloch<sup>32,33</sup> has shown that the magnetic susceptibilities of compounds with  $^2T_2$  and  $^5T_2$  ground terms are significantly affected by configuration interactions, a factor not considered in the treatment employed here.

$\text{H}[\text{Fe}(\text{bipy})(\text{CN})_4]$ . A coordinate system consistent with the symmetry of  $\text{Fe}(\text{bipy})(\text{CN})_4^-$  is shown in Figure 4. Quantizing in  $C_{2v}$  symmetry the  $t_{2g}$  orbitals expressed in real form are  $|xy\rangle$ ,  $|xz\rangle$ , and  $|z^2 - y^2\rangle$ . The temperature-independent contributions are calculated in the manner described previously, with  $\text{CN}^-$  considered as a stronger  $\sigma$  donor than 2,2'-bipyridine. It is found that  $q_1$  should be positive and that  $\eta_1 = -3$ .

The quadrupole splitting data were fitted in a manner similar to that of  $[\text{Fe}(\text{bipy})_2(\text{CN})_2]\text{ClO}_4$ . Initially it was assumed that  $\beta^2/\alpha^2 = 1.0$ . Those solutions which are in reasonable agreement with the quadrupole splitting results and give a positive  $q_1$  are shown in Table IV. The calculated  $g$  values

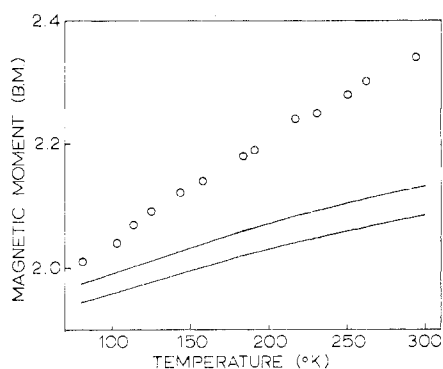


Figure 3. The temperature dependence of the average magnetic moment of  $[\text{Fe}(\text{bipy})_2(\text{CN})_2]\text{ClO}_4$  obtained from B. N. Figgis, J. Lewis, F. E. Mabbs, and G. A. Webb, *J. Chem. Soc. A*, 422 (1966). The bottom line gives the calculated moments for  $\zeta = 150 \text{ cm}^{-1}$ ,  $\Delta = 1200 \text{ cm}^{-1}$ ,  $\epsilon = 1000 \text{ cm}^{-1}$ , and  $k = 1.0$ . The top line is calculated with  $\zeta = 150 \text{ cm}^{-1}$ ,  $\Delta = 1000 \text{ cm}^{-1}$ ,  $\epsilon = 800 \text{ cm}^{-1}$ , and  $k = 1.0$ .

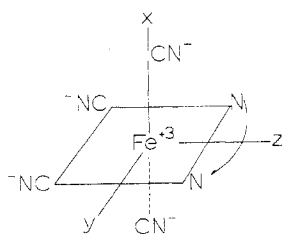


Figure 4. The coordinate system for  $[\text{Fe}(\text{bipy})(\text{CN})_4]^-$ .

are also shown in Table IV. In this calculation it was assumed that  $B = 650 \text{ cm}^{-1}$ ,  $E = 30,000 \text{ cm}^{-1}$ , and  $\zeta_{\sigma\pi} = 120 \text{ cm}^{-1}$ . There are three ranges which give reasonable agreement between the esr and quadrupole splitting results: (1)  $\zeta = 100\text{--}150 \text{ cm}^{-1}$ ,  $\Delta/\zeta = -3$  to  $-4$ ,  $\epsilon = 300\text{--}400 \text{ cm}^{-1}$  with  $\beta^2 = 0.2\text{--}0.3$ ; (2)  $\zeta = 150 \text{ cm}^{-1}$ ,  $\Delta/\zeta = -3$  to  $-4$ ,  $\epsilon \approx -400 \text{ cm}^{-1}$  with  $\beta^2 \approx 0.5$ ; (3)  $\zeta = 150\text{--}200 \text{ cm}^{-1}$ ,  $\Delta/\zeta \approx 3$ ,  $\epsilon = -100$  to  $-200$ , and  $\beta^2 \approx 0.5$ . The first solution with  $\Delta$  negative and  $\epsilon$  positive appears to be the most likely solution. Previous work<sup>9</sup> suggests that  $\text{CN}^-$  causes greater  $t_{2g}$  orbital expansion and lower spin-orbit coupling constants than 2,2'-bipyridine. It would therefore be expected that  $\text{H}[\text{Fe}(\text{bipy})(\text{CN})_4]$  would exhibit  $\zeta$  and  $\beta^2$  values lower than those observed for  $[\text{Fe}(\text{bipy})_2(\text{CN})_2]\text{ClO}_4$ . Only solution (1) is consistent with this expectation. In addition, the  $\zeta$  and  $\beta^2$  values are in agreement with a weighted average of the values observed for  $\text{Fe}(\text{CN})_6^{3-2}$  and  $\text{Fe}(\text{bipy})_3^{3+}$ .<sup>9</sup> The  $t_{2g}$  orbital scheme suggested by solution (1) is given in Figure 5. The  $q$  and  $\eta$  values at  $300^\circ$  have been calculated for solutions (1), (2), and (3). Solution (1) gives  $q$  negative and  $\eta$  small ( $\eta < 0.2$ ). Solutions (2) and (3) give  $q$  positive with  $\eta$  relatively large ( $\eta > 0.3$ ). A magnetic perturbation Mossbauer spectrum would be useful to substantiate our assignment.

The  $\text{H}[\text{Fe}(\text{bipy})(\text{CN})_4]$  results were also tested for the effect of anisotropic radial expansion. Setting  $\beta^2/\alpha^2 = 0.75$  and  $\beta^2/\alpha^2 = 1.25$ , it is found that only  $1/2e^2Qq_1$  and  $\beta^2$  are changed significantly. The ranges of  $\zeta$ ,  $\Delta$ , and  $\epsilon$  remain close to those given in Table IV. The average of  $\beta^2$ ,  $\alpha^2$ , is changed by less than 0.10 from the  $\beta^2$  value given in Table IV. In order to test the sensitivity of the results to assumptions regarding the magnitude of the various "lattice" contributions to the EFG tensor, the data were fitted with  $\eta_1 = -2.0$ . The results remain close to those given in Table IV. The  $\beta^2$  value is changed by less than 0.10.

The results presented here must be considered in view of the inadequacies of the methods of analysis. The epr spectra are broad resulting in imprecise  $g$  values. The theoretical analysis of the epr data is probably not complete. In the analysis of the quadrupole splitting data, it is assumed that

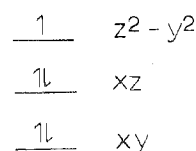


Figure 5. The relative energy of the cubic  $t_{2g}(\pi^*)$  orbitals consistent with solution set (1).

the distortion parameters are temperature independent in the range  $80\text{--}300^\circ$ . The latter assumption appears reasonable<sup>9</sup> but some temperature dependence cannot be completely ruled out. Agreement with the magnetic susceptibility data is not obtained. However, it has been found possible to interpret the epr and quadrupole splitting data of  $[\text{Fe}(\text{bipy})_2(\text{CN})_2]\text{ClO}_4$  and  $\text{H}[\text{Fe}(\text{bipy})(\text{CN})_4]$  in a consistent manner, which is in reasonable accord with similar studies of  $\text{K}_3\text{Fe}(\text{CN})_6$  and  $\text{Fe}(\text{bipy})_3(\text{ClO}_4)_3$ .

These results indicate that the cubic  ${}^2T_{2g}$  ground term of the trigonally distorted  $[\text{Fe}(\text{bipy})_2(\text{CN})_2]\text{ClO}_4$  exhibits an axial splitting of about  $1000 \text{ cm}^{-1}$  with a superimposed rhombic splitting of slightly lower magnitude. The magnitude of the spin-orbit coupling constant is about  $150 \text{ cm}^{-1}$ . This analysis suggests that the compound  $\text{H}[\text{Fe}(\text{bipy})(\text{CN})_4]$  exhibits a tetragonal distortion of about  $-400 \text{ cm}^{-1}$  with a somewhat smaller superimposed rhombic distortion. The spin-orbit coupling constant appears to have a magnitude of between  $100$  and  $150 \text{ cm}^{-1}$ .

**Acknowledgment.** Acknowledgment is made to the donors of the Petroleum Research Fund, administered by the American Chemical Society, for support of this research.

**Registry No.**  $[\text{Fe}(\text{bipy})_2(\text{CN})_2]\text{ClO}_4$ , 15154-53-7;  $[\text{Fe}(\text{phen})_2(\text{CN})_2]\text{ClO}_4$ , 15672-20-5;  $[\text{Fe}(\text{bipy})_2(\text{CN})_2]\text{NO}_3$ , 15225-35-1;  $[\text{Fe}(\text{phen})_2(\text{CN})_2]\text{NO}_3$ , 14783-56-3;  $\text{H}[\text{Fe}(\text{bipy})(\text{CN})_4]$ , 31307-03-6;  $\text{H}[\text{Fe}(\text{phen})(\text{CN})_4]$ , 12112-06-0.

## References and Notes

- W. T. Oosterhuis and G. Long, *Phys. Rev.*, **178**, 439 (1969).
- P. B. Merrithew and A. J. Modestino, *J. Amer. Chem. Soc.*, **94**, 3361 (1972).
- R. M. Golding, *Mol. Phys.*, **12**, 13 (1967).
- R. M. Golding and H. J. Whitfield, *Trans. Faraday Soc.*, **62**, 1713 (1966).
- R. L. Martin and I. A. G. Roos, *Aust. J. Chem.*, **24**, 2231 (1971).
- W. M. Reiff and D. Szymanski, *Chem. Phys. Lett.*, **17**, 288 (1972).
- P. B. Merrithew and P. G. Rasmussen, *Inorg. Chem.*, **11**, 325 (1972).
- W. M. Reiff, *Chem. Phys. Lett.*, **8**, 297 (1971).
- P. B. Merrithew, C.-C. Lo, and A. J. Modestino, *Inorg. Chem.*, **12**, 1927 (1973).
- C. D. Burbridge, D. M. Goodgame, and M. Goodgame, *J. Chem. Soc. A*, 349 (1967).
- P. B. Merrithew, P. G. Rasmussen, and D. H. Vincent, *Inorg. Chem.*, **10**, 1401 (1971).
- P. B. Merrithew, J. J. Guerrero, and A. J. Modestino, *Inorg. Chem.*, **13**, 644 (1974).
- W. M. Reiff and R. E. DeSimone, *Inorg. Chem.*, **12**, 1793 (1973).
- A. A. Schilt, *J. Amer. Chem. Soc.*, **82**, 3000 (1960).
- J. F. Ullrich, Ph.D. Thesis, University of Michigan, 1967.
- R. Ingalls, *Phys. Rev. A*, **133**, 787 (1964).
- B. Bleaney and M. C. M. O'Brien, *Proc. Phys. Soc., London, Sect. B.*, **69**, 1205 (1956).
- J. S. Griffith, "The Theory of Transition-Metal Ions," Cambridge University Press, London, 1961, p 364.
- J. C. Travis in "An Introduction to Mossbauer Spectroscopy," Plenum Press, New York, N. Y., 1971, p 77.
- G. M. Bancroft, M. J. Mays, and B. E. Prater, *J. Chem. Soc. A*, 956 (1970).
- G. M. Bancroft, R. E. B. Garrod, and H. G. Maddock, *J. Chem. Soc. A*, 3165 (1971).
- R. R. Berrett and B. W. Fitzsimmons, *J. Chem. Soc. A*, 525 (1967).
- C. J. Ballhausen, "Introduction to Ligand Field Theory," McGraw-Hill, New York, N. Y., 1962, p 166.
- N. J. Hill, *J. Chem. Soc., Faraday Trans.*, **2**, **68**, 427 (1972).
- J. H. Van Vleck, "The Theory of Electric and Magnetic Susceptibilities," Oxford University Press, London, 1932, p 192.
- B. N. Figgis, *Trans. Faraday Soc.*, **57**, 198 (1961).
- N. E. Erickson, Ph.D. Thesis, University of Washington, 1964.
- C. S. Naiman, *J. Chem. Phys.*, **35**, 323 (1961).
- R. D. Feltham and W. Silverthorn, *Inorg. Chem.*, **9**, 1207 (1970).

- (30) T. M. Dunn, *Trans. Faraday Soc.*, **57**, 1441 (1961).  
 (31) B. N. Figgis, J. Lewis, F. E. Mabbs, and G. A. Webb, *J. Chem. Soc. A*, 422 (1966).

- (32) M. Gerloch, *J. Chem. Soc. A*, 2023 (1968).  
 (33) M. Gerloch, J. Lewis, G. G. Phillips, and P. N. Quedstedt, *J. Chem. Soc. A*, 1941 (1970).

Contribution from the Department of Chemistry,  
 University of Wisconsin, Madison, Wisconsin 53706

## The Transition Metal–Isocyanide Bond. An Approximate Molecular Orbital Study

ALLEN C. SARAPU and RICHARD F. FENSKE\*

Received May 16, 1974

AIC40314+

The bonding properties of methyl isocyanide in transition metal complexes are examined *via* approximate molecular orbital calculations on the series of complexes  $\text{Mn}(\text{CO})_{5-n}(\text{CNCH}_3)_n\text{Br}$ ,  $n = 0-4$ ,  $\text{Mn}(\text{CO})_{6-n}(\text{CNCH}_3)_n^+$ ,  $n = 0-6$ , and  $\text{Fe}(\text{CNCH}_3)_6^{2+}$ . A force constant analysis is presented which, in conjunction with the molecular orbital results, shows that both  $\sigma$ - and  $\pi$ -bonding changes in the metal to isocyanide bond can influence observed stretching frequencies. The antibonding behavior of the  $7a_1$  orbital, the carbon "lone pair" in methyl isocyanide, helps explain the observed increase in  $\nu_{\text{CN}}$  values for bound methyl isocyanide compared to the free ligand in many metal complexes even though there is significant back-bonding to the ligand. We also find that for the cationic manganese species electrochemical potentials for the  $+1 \rightarrow +2$  oxidation process correlate extremely well with calculated highest occupied molecular orbital (HOMO) energies. These results confirm the importance of including near-neighbor interactions in an approximate molecular orbital scheme.

### Introduction

In the past few years there has been considerable research in the field of isocyanides as ligands in transition metal complexes.<sup>1,2</sup> In such complexes isocyanides are generally thought of as being capable of extensive back-bonding in a manner analogous to that of carbonyl.<sup>3</sup> Recently we published the results of an X-ray diffraction and molecular orbital study on  $\text{Mn}(\text{CO})_3(\text{CNCH}_3)_2\text{Br}$ , which showed that significant back-bonding to the methyl isocyanide ligand does occur, even in competition with carbonyl.<sup>4</sup> In order better to understand the consequences of the bonding of methyl isocyanide to a transition metal and the physical and chemical properties of the resulting complexes we have undertaken molecular orbital studies on the series of complexes  $\text{Mn}(\text{CO})_{5-n}(\text{CNCH}_3)_n\text{Br}$ ,  $n = 0-4$ ,  $\text{Mn}(\text{CO})_{6-n}(\text{CNCH}_3)_n^+$ ,  $n = 0-6$ , and  $\text{Fe}(\text{CNCH}_3)_6^{2+}$ . These complexes allow comparison of carbonyl and isocyanide ligands competing in varied molecular environments. In addition, comparison of some of these complexes with their carbonyl or cyanide analogs, for example  $\text{Mn}(\text{CO})_6^+$ ,  $\text{Mn}(\text{CN})_6^{5-}$ ,  $\text{Mn}(\text{CO})_5\text{CN}$ , and  $\text{Mn}(\text{CO})_5\text{CNCH}_3^+$ , provides an opportunity to contrast carbonyl, cyanide, and isocyanide bonding.

### Molecular Orbital Calculations

**Method.** The approximate, nonparameterized molecular orbital method has been described previously.<sup>5</sup> Choice of wave functions and bond distances is described below. All calculations were carried out using the MEDIEVAL series of programs written in these laboratories for the Univac 1108 computer at the Academic Computing Center, Madison, Wis.<sup>6</sup>

**Basis Functions.** Clementi's double- $\zeta$  functions for neutral atoms were used for carbon, oxygen, and nitrogen,<sup>7</sup> except that the  $N(-1)$  functions were used for cyanide nitrogen.<sup>8</sup> Choice of wave functions is made consistent with the resulting atomic charges calculated *via* a Mulliken population analysis<sup>9</sup> in all cases. The  $1s$  and  $2s$  functions were curve-fit to single  $\zeta$  using the maximum-overlap criterion, while maintaining their orthogonality.<sup>10</sup> For bromine the "best atom" functions of Clementi and Raimondi were used,<sup>11</sup> after Schmidt orthogonalization to ensure that all one-center overlaps are zero. For hydrogen, an exponent of 1.16 was used, which corresponds to the minimum energy exponent for methane.<sup>12</sup>

For manganese the  $1s-3d$  functions were taken from the results of Richardson, *et al.*<sup>13</sup> For the  $3d$  case we used the function corresponding to the  $\text{Mn}^+$  ( $3d^6$ ) configuration.  $4s$  and  $4p$  orbitals for manganese were constructed in a manner

Table I. Bond Distances and Angles

Distances, Å			
Mn–Co	1.79 (trans to Br only)	C≡O	1.128
Mn–CO	1.83 (all others)	C≡N(isocyanide)	1.166
Mn–CNCH <sub>3</sub>	1.97	N–CH <sub>3</sub>	1.424
Mn–Br	2.537	C–H	1.102
Fe–CNCH <sub>3</sub>	1.90	C≡N(cyanide)	1.16
Mn–CN	1.97		

Angles			
C–N–C	180°	N–C–H	109° 28'

described previously by maximizing their overlap with the carbonyl carbon atom.<sup>14</sup> Iron functions were chosen in the same way. A more detailed discussion of the method for obtaining the basis functions, including the list of orbital exponents and coefficients for the various functions, is available.<sup>15</sup>

**Bond Parameters.** Free-ligand bond distances for  $\text{CNCH}_3$ <sup>16</sup> and  $\text{CO}$ <sup>17</sup> were used in this work. For cyanide a value of 1.16 Å was used as in previous work.<sup>18,19</sup> Structural studies confirm that the ligand values for the bound case differ only slightly from the free values. The metal to ligand distances were chosen as follows. For the manganese complexes we referred to the crystal structure results for  $\text{Mn}(\text{CO})_3(\text{CNCH}_3)_2\text{Br}$ .<sup>4</sup> Thus, the Mn–CO distance for a carbonyl trans to bromine was taken as 1.79 Å, while for all other cases Mn–CO was maintained at 1.83 Å, the average of the equatorial carbonyl distances in the crystal structure. Manganese to methyl isocyanide distances were maintained at 1.97 Å, also the average value. The Mn–Br distance was taken as 2.537 Å.

For the  $\text{Fe}(\text{CNCH}_3)_6^{2+}$  calculation we took note of our previous observation that there is a correspondence of metal to methyl isocyanide bond lengths and metal to cyanide bond lengths.<sup>4</sup> Therefore we chose an Fe–CNCH<sub>3</sub> distance equal to the Fe–CN distance of 1.90 Å in  $\text{Na}_2\text{Fe}(\text{CN})_5\text{NO}\cdot 2\text{H}_2\text{O}$ .<sup>20</sup>

For the manganese cyanide complexes, the Mn–CN distance was taken as 1.97 Å, the same value as for the Mn–CNCH<sub>3</sub> distance. An advantage of maintaining the Mn–CN value the same as the Mn–CNCH<sub>3</sub> distance is that differences in bonding observed for the two ligands can be attributed to electronic changes within the complex, rather than apparently minor bond distance changes. The value of 1.97 Å compares favorably to the mean manganese to carbon distance of 1.98 Å in  $\text{K}_3\text{Mn}(\text{CN})_5\text{NO}\cdot 2\text{H}_2\text{O}$ .<sup>21</sup> Table I summarizes all the bond distances used.

**Free-Ligand Results.** While the calculations are carried out in an atomic basis set, it is more useful for the interpretation